PROPERTIES OF Eu^{3+} LUMINESCENCE IN THE MONOCLINIC $Ba_2MgSi_2O_7$

SHANSHAN YAO, #LIHONG XUE, YOUWEI YAN

State Key Laboratory of Materials Processing and Die & Mould Technology, College of Materials Science and Engineering, Huazhong University of Science & Technology, Wuhan 430074, P.R. China

#E-mail: xuelh@mail.hust.edu.cn

Submitted September 27, 2010; accepted July 3, 2011

Keywords: Optical materials, Crystal structure, Luminescence, Optical properties

Red-emitting phosphors $Ba_{2-x}MgSi_2O_7$: Eu_x^{3+} was prepared by combustion-assisted synthesis method and an efficient red emission under near-ultraviolet (UV) was observed. The luminescence and crystallinity were investigated using luminescence spectrometry and X-ray diffractometer. The emission spectrum shows that the most intense peak is located at 614 nm, which corresponds to the $^5D_0 \rightarrow {}^7F_2$ transitions of Eu^{3+}. The phosphor has two main excitation peaks located at 394 and 465 nm, which match the emission of UV and blue light-emitting diodes, respectively. The effect of Eu^{3+} concentration on the emission spectrum of $Ba_2MgSi_2O_7$:Eu^{3+} phosphor was studied. The results showed that the emission intensity increased with increasing Eu^{3+} concentration, and then decreased because of concentration quenching. The critical quenching concentration of Eu^{3+} in $Ba_2MgSi_2O_7$: Eu^{3+} phosphor is about 0.05 mol. The mechanism of concentration quenching of $Ba_2MgSi_2O_7$: Eu^{3+} luminescence is energy transfer between Eu3+ ions casued by the dipole-dipole interaction.

INTRODUCTION

The White-light emitting diodes (LEDs) have attracted considerable attention as a solid-state light source [1,2]. Nowadays, many materials for fluorescent lamp emitting green, yellow and red lights have been explored in order to develop phosphors converted W-LEDs [3,4]. Three-band white LEDs maintain a very high color rendering index and were believed to offer the greatest potential for high efficiency solid-state lighting [5]. For excellent color-rendering index, both methods need efficient red phosphors that should have the excitation wavelength matching with the emission wavelength of the blue LEDs (λ_{em} = 440-470 nm) or the UV/violet LEDs (λ_{em} = 350-420 nm). The presently used red phosphors for blue and near-UV/violet GaN-baded LED are commercially still limited to divalent Eu ions activated alkaline earth binary sulfides and Y_2O_2S: Eu^{3+}, respectively. However, these sulfide-based phosphors are chemically unstable and the lifetime of these materials are inadequate, and their luminescent intensities very low relative to blue and green phosphor. Hence, the search for a stable red phosphor with intense absorption in the near-UV/blue spectra region is an urgent need to increase the overall white light efficiency and lifetime [6, 7].

In recent times, Eu^{3+}-doped hardystonites and akermanites have been extensively investigated as red phosphors because of their chemical stability. The intensities of Eu^{3+} excitation lines at around 394 and 465 nm are enhanced obviously in these materials compared with most other Eu^{3+}-doped phosphors [8-13]. To the best our knowledge, there is no report on the research of $Ba_2MgSi_2O_7$: Eu^{3+} for potential application as a red phosphor. Here we report on the synthesis and characterization of red emitting $Ba_2MgSi_2O_7$: Eu^{3+} powders by a combustion-assisted synthesis method and investigate their luminescent properties.

EXPERIMENTAL

Synthesis

Powder samples with the general formula $Ba_{2-x}MgSi_2O_7$: Eu_x^{3+} (x = 0-0.09) phosphor were prepared by the combustion-assisted synthesis method. The starting materials were $Ba(NO_3)_2$ (analytical grade), $Mg(NO_3)_2 \cdot 6H_2O$ (analytical grade), $Si(OC_2H_5)_4$ (analytical grade), Eu_2O_3 (99.99%), NH_2CONH_2 (analytical grade) and H_3BO_3 (analytical grade). NH_2CONH_2 was added as a fuel and H_3BO_3 was a flux, respectively. Eu_2O_3 was dissolved in HNO_3 to convert into $Eu(NO_3)_3$ solution

completely. The appropriate molar ratio of $Ba(NO_3)_2$, $Mg(NO_3)_2 \cdot 6H_2O$, $Eu(NO_3)_3$, NH_2CONH_2 and H_3BO_3 were dissolved in a minimum amount of distilled water to get a clear solution. Then a stoichiometric amount of $Si(OC_2H_5)_4$ dissolved in ethanol was added dropwise into the above solution under vigorous stirring. $Si(OH)_4$ was formed by the hydrolysis of $Si(OC_2H_5)_4$ as follows:

$$nSi(OC_2H_5)_4 + H_2O \rightarrow nSi(OH)_4 + 4nC_2H_5OH$$

The mixture solution was allowed to react at 80°C for 2 h to obtain a homogenous solution. And then the solution was introduced into a muffle furnace preheated at 600°C. Within a few minutes, the solution boiled and was ignited to produce a self-propagating flame. The product obtained was post-annealed at 1000°C for 3 h.

Sample characterization

The synthesized phosphors were ground to powder and sieved by 200 mesh for characterization. The crystal phase of the synthesized powders prepared in the process was characterized by X-ray powder diffraction using an X′ Pert PRO X-ray diffractometer having a Cu Kα radiation (λ = 1.5406 Å) at 40 kV tube voltage and 40 mA tube current. The XRD patterns collected in the range of $10° \leq 2\theta \leq 90°$. The excitation and emission spectra were performed on a RF-5301 fluorescence spectrophotometer equipped with a xenon discharge lamp as an excitation source. The excitation and emission slits were set to 3.0 nm. All the above measurements were taken at room temperature.

The chromaticity coordinates were obtained according to the Commission International de l'Eclairage (CIE) using a Spectra Lux Software v.2.0 Beta [14, 15].

RESULTS AND DISCUSSION

Crystal structure

The crystal structure of $Ba_2MgSi_2O_7$ is composed of a tetrahedron framework, $[Mg_2Si_2O_7]$, and isolated barium atoms. Two silicon tetrahedral are connected by sharing an oxygen, forming a di-silicate group Si_2O_7[16]. All of the barium atoms are located in the channel and coordinated by oxygen atoms in both the structures (Figure 1).

Phase formation

The stoichiometric composition of the redox mixture was calculated based on the total oxidizing and reducing valence of the oxidizer and the fuel. For the combustion synthesis of oxides, metal nitrates are employed as oxidizer and urea is employed as a reducer [17]. With the calculation of oxidizer to fuel ratio, the elements were assigned formal valences as follows: Ba = +2, Mg = +2, Eu = +3, Si = +4, B = +3, C = +4, H = +1, O = -2 and N = 0. Accordingly, the oxidizer and fuel values for various reactants are as given below:

$$\begin{array}{cccccc} 19.5Ba(NO_3)_2 & + Mg(NO_3)_2 & + 0.05Eu(NO_3)_3 & + Si(OH)_4 & + H_3BO_3 & + CO(NH_2)_2 \\ -19.5 & -10 & -0.75 & 0 & 0 & +6 \end{array}$$

For complete combustion, the oxidizer and the fuel serve as a numerical coefficient for the stoichiometric balance, so that the equivalence ratio is equal to unity (total oxidizing valency / total reducing valency (O/F) = 1), and the maximum energy is released [18]. Thus, the molar ratio of the reactants taken is 1.95:1:0.05:2:0.06:5 for $Ba(NO_3)_2$:$Mg(NO_3)_2$:$Eu(NO_3)_3$:$Si(OH)_4$:H_3BO_3:$CO(NH_2)_2$. Owing to the combustion process, the solution boiled and dehydrated, followed by decomposition with escape of large amounts of gases (oxides of carbon, nitrogen and ammonia), then spontaneous ignition occurred and underwent smoldering combustion with enormous swelling. The whole combustion process was over within less than 5 min. After the combustion, the ashes were cooled to room temperature. Finally, the ashes obtained were post-annealed at 1000°C for 3 h.

The XRD patterns of our samples, $Ba_{2-x}MgSi_2O_7$:Eu_x^{3+} (x = 0-0.09), are shown in Figure 2, which indicated that doped Eu^{3+} ions have no obvious influence on the structure of the host. A pure phase of the monoclinic $Ba_2MgSi_2O_7$ has formed in these samples. The fraction peak positions and the relative intensities of the prepared samples are well matched with that in the literature. The layered structure, with the following cell parameters: a = 8.4128 Å, b = 10.7101 Å, c = 8.4387 Å, β = 110.71°, consists of discrete $[Si_2O_7]^{6-}$ units connected by tetrahedral coordinated Mg^{2+} and eight-coordinated Ba^{2+} ions [16]. No trace of the previously reported tetragonal $Ba_2MgSi_2O_7$ phase could be observed in the XRD patterns [19]. In this work, the structure of monoclinic $Ba_2MgSi_2O_7$ with space group C2/c was taken as the starting model for the synthesized phosphors.

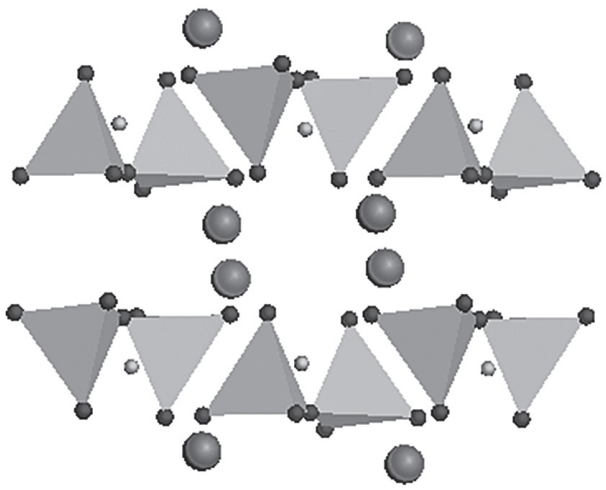

Figure 1. Crystal structure of $Ba_2MgSi_2O_7$.

The lattice parameters listed in Table 1 shows that there is good agreement between the literature and the prepared $Ba_2MgSi_2O_7$ and $Ba_{2-x}MgSi_2O_7$: Eu_x^{3+} (x = 0.01-0.09) samples values, suggesting that the method starting form the silicates are successfully applied here. Meanwhile, it is clear that the Eu^{3+} doping ions do not change the general structure.

An acceptable percentage difference in ion radii between doped and substituted ions must not exceed 30 % [20]. The calculations of the radius percentage difference (D_r) between the doped ions (Eu^{3+}) and the possible substituted ions (Ba^{2+}, Mg^{2+}, Si^{4+}) in $Ba_2MgSi_2O_7$ are summarized in Table 2. The values are based on the following formula

$$Dr = \frac{Rm(CN) - Rd(CN)}{Rm(CN)}$$

where *CN* is the coordination number, $R_m(CN)$ is the radius of host cation, and $R_d(CN)$ is the radius of doped ion. The value of Dr between Eu^{3+} and Ba^{2+} on eight-coordinated sites is 24.93 %. While that between Eu^{3+} and Mg^{2+} (or Si^{4+}) is -66.14 % (or-264.23%). Obviously, the doping ions of Eu^{3+} will clearly substitute the barium sites.

As trivalent Eu^{3+} ions are doped into $Ba_2MgSi_2O_7$, they would non-equavalently replace the alkaline earths ions. In order to keep the charge balance, two Eu^{3+} ions would be needed to substitute for three alkaline earths ions (the total charge of two trivalent Eu^{3+} ions is equal to that of three alkaline earths ions). Hence, one vacancy defect of V_{Ba}'' with two negative charges, and two positive defects of $Eu_{Ba}^{\cdot}$ would be created by each substitution of every two Eu^{3+} ions in the compound. The vacancy V_{Ba}'' would act as a donor of electrons, while the two $Eu_{Ba}^{\cdot}$ defects become acceptors of the electrons. Consequently, the negative charges in the vacancy defects of V_{Ba}'' would be transferred to the Eu^{3+} sites. The whole process can be expressed by the following equation [22]:

$$3Ba^{2+} + 2Eu^{3+} \rightarrow V''_{Ba} + 2Eu_{Ba}^{\cdot}$$

$$V''_{Ba} \rightarrow V_{Ba}^{x} + 2e$$

$$2Eu_{Ba}^{\cdot} + 2e \rightarrow 2Eu_{Ba}^{x}$$

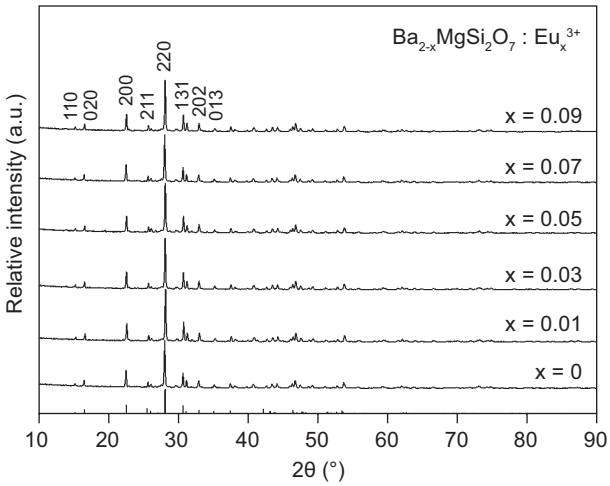

Figure 2. XRD patterns of $Ba_{2-x}MgSi_2O_7$: Eu_x^{3+} (x = 0, 0.01, 0.03, 0.05, 0.07, and 0.09) phosphors.

Luminescent properties

The effect of Eu^{3+} concentration on emission intensity of $Ba_2MgSi_2O_7$: Eu^{3+} phosphor excited by different excitation wavelengths is shown in Figure 3, in which the Eu^{3+} concentration varies from 0.01 mol to 0.09 mol. It can be observed that the emission intensities increase with increasing Eu^{3+} concentration, and then decrease because of the concentration quenching, and reach the maximal value at 0.05 mol.

Table 1. Lattice parameters values of $Ba_{2-x}MgSi_2O_7$: Eu_x^{3+} (x = 0, 0.01, 0.03, 0.05, 0.07, 0.09) phosphors calculated from the XRD pattern.

Samples	*a* (Å)	*b* (Å)	*c* (Å)	*V* (Å^3)
$Ba_2MgSi_2O_7$ (this work)	8.2059	10.4516	8.3002	698.82
$Ba_{1.99}MgSi_2O_7$: $Eu_{0.01}^{3+}$	8.1996	10.4433	8.2920	695.27
$Ba_{1.97}MgSi_2O_7$: $Eu_{0.03}^{3+}$	8.1822	10.4195	8.2852	693.46
$Ba_{1.95}MgSi_2O_7$: $Eu_{0.05}^{3+}$	8.1613	10.3976	8.2621	691.83
$Ba_{1.93}MgSi_2O_7$: $Eu_{0.07}^{3+}$	8.1436	10.3811	8.2510	689.52
$Ba_{1.91}MgSi_2O_7$: $Eu_{0.09}^{3+}$	8.1288	10.3679	8.2303	687.62
Reference [16]	8.4128	10.7101	8.4387	711.20

Table 2. Ionic radii difference percentage (Dr) between matrix cations and doped ions.

		Dr = [Rm(CN)-Rd(CN)]/Rm(CN) (%)		
Doped ions	Rd(CN) (Å)	$R_{Ba}^{2+}(8)$ = 1.42 (Å)	$R_{Mg}^{2+}(4)$ = 0.57 (Å)	$R_{Si}^{4+}(4)$ = 0.26 (Å)
Eu^{3+}	0.947 (6)		- 66.14	-264.23
	1.066 (8)	24.93		

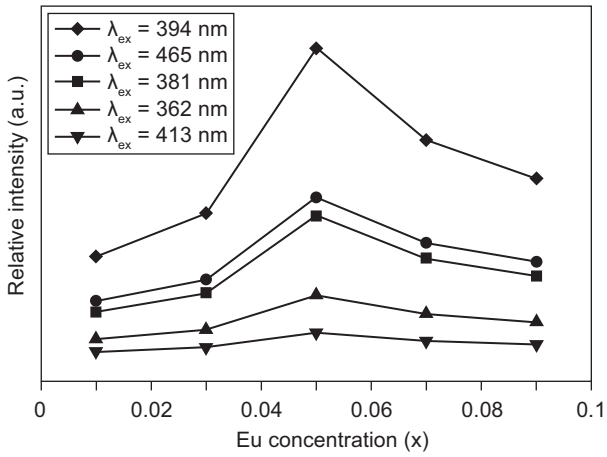

Figure 3. Emission intensity vs europium concentration (x) of $Ba_{2-x}MgSi_2O_7$: Eu_x^{3+} phosphor under various excitation wavelengths (λ_{em} = 614 nm).

The emission intensity (I) per activator ion follows the equation [22, 23]:

$$\frac{1}{x} = K[1+\beta(x)^{Q/3}]^{-1}$$

where x is the activator concentration; Q = 6, 8, 10 for dipole-dipole(d-d), dipole-quadrupole(d-q), quadrupole-quadrupole(q-q) interactions, respectively; and K and β are constant for the same excitation conditions for a given host crystal. The critical concentration of Eu^{3+} has been determined to be 0.05 mol. The dependence of the emission intensity of $Ba_2MgSi_2O_7$: Eu^{3+} phosphor excited at 394 nm as a function of the corresponding concentration of Eu^{3+} for concentration greater than the critical concentration is determined. The polt of lg $I/x_{Eu^{3+}}$ as a function of lg $x_{Eu^{3+}}$ in $Ba_{2-x}MgSi_2O_7$: Eu_x^{3+} phosphor are shown in Figure 4. It can be seen that dependence of lg $x_{Eu^{3+}}$ on lg $I/x_{Eu^{3+}}$ is linear and the slope is -1.989. The value of Q can be calculated as 5.967, which is close to 6. The result indicates that the concentration self-quenching mechanism of Eu^{3+} luminescence in $Ba_2MgSi_2O_7$ is the d-d interaction.

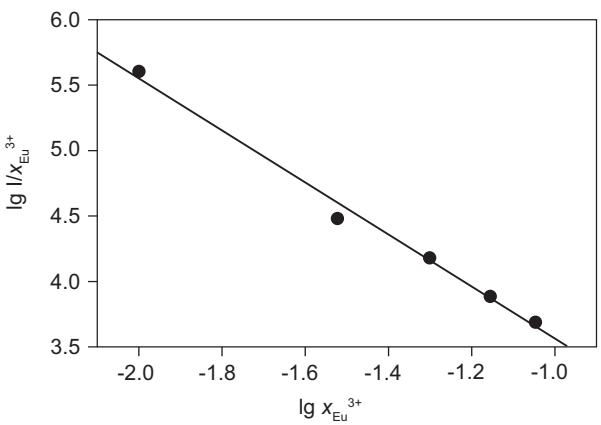

Figure 4. Plot of lg $I/x_{Eu^{3+}}$ as a function of 1 lg $x_{Eu^{3+}}$ in $Ba_{2-x}MgSi_2O_7$: Eu_x^{3+} phosphors (λ_{ex} = 394 nm).

The excitation spectra of $Ba_{1.95}MgSi_2O_7$: $Eu_{0.05}^{3+}$ is measured in the wavelength range of 260-465 nm by monitoring with the intense red emission located at 614 nm (Figure 5a). The excitation spectra consist of two intense bands at 394 and 465 nm in addition to three relatively weak bands peaking about 362, 381, and 413 nm. The bands peaking around 362, 394 and 465 nm are assigned to transition from the $^7F_0$ level to the $^5D_4$, $^5L_6$, and $^5D_2$ levels of f-f transitions of Eu^{3+}, respectively. On the other hand, rest of the bands peaking around 381 and 413 nm are assigned to the transitions from the thermal populated $^7F_1$ level to the $^5F_4$ and $^5L_3$ [24, 25]. The strong broad band peaking at 394 nm and the narrow band at 465 nm correspond to the characteristic f-f transitions of Eu^{3+} within its $^4f_6$ configuration. Figure 5b shows the emission spectral of as-synthesized Eu^{3+}-doped $Ba_2MgSi_2O_7$ phosphors. The spectrum exhibits two main peaks centered at 591 and 614 nm, which come from the transitions of $^5D_0 \rightarrow {}^7F_1$ and $^5D_0 \rightarrow {}^7F_2$, respectively. The most intense emission is the $^5D_0 \rightarrow {}^7F_2$ transition located at 614 nm, corresponding to the red emission, in good accordance with the Judd-Ofelt theory [24]. Therefore, strong red emission can be observed. The main excitation peaks indicate the phosphor is very suitable for a color converter using UV lights as the primary light source. It can be used as a red phosphor excited by UV-LED chip and would have applications in the solid-state lighting field.

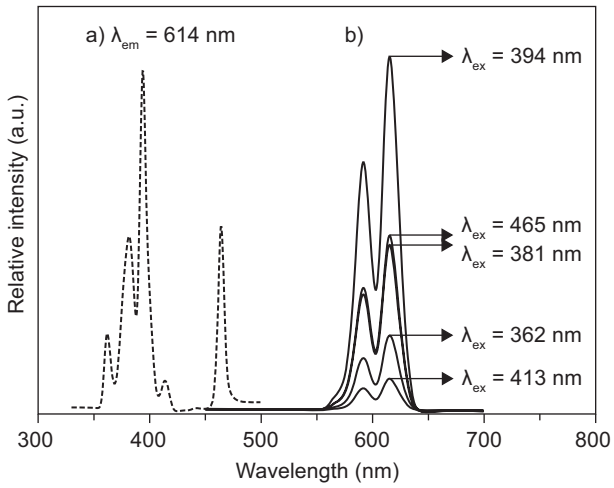

Figure 5. Photoluminescence spectra of $Ba_{1.95}MgSi_2O_7$: $Eu_{0.05}^{3+}$ phosphor.

Color purity can be visualized in the chromaticity diagram (Figure 6) as blue, red, and green regions, using the color coordinates of the luminescent material emission. So, from the luminescence emission spectra of $Ba_{1.95}MgSi_2O_7$:$Eu_{0.05}^{3+}$ sample we obtained the chromaticity coordiantes with the aid of the Spectra Lux Software v.2.0 Beta [14]. For any given color there is one setting for each three number X, Y and Z known as

tristimulus values that will produce a match. Based on emission spectra of $Ba_{1.95}MgSi_2O_7$:$Eu_{0.05}^{3+}$ sample, the (x, y) color coordinates were determined with the following values (x, y) = (0.623, 0.376).

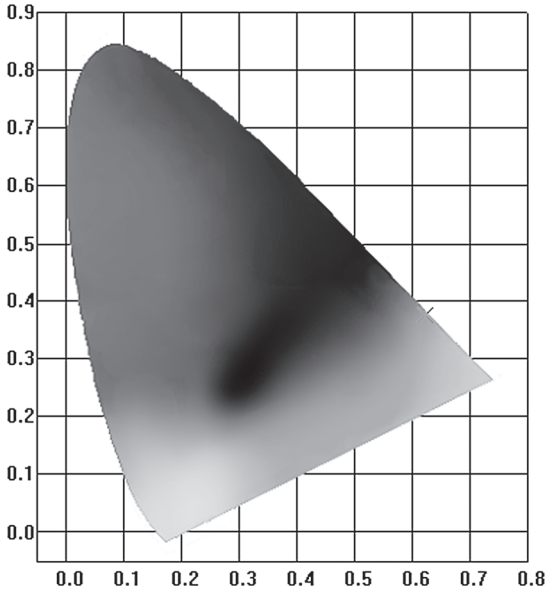

Figure 6. Chromaticity coordinates calculated from emission spectra of the $Ba_{1.95}MgSi_2O_7$: $Eu_{0.05}^{3+}$, (λ_{ex} = 394 nm).

CONCLUSIONS

The monoclinic $Ba_2MgSi_2O_7$: Eu^{3+} phosphors were synthesized by combustion-assisted synthesis method and its luminescent properties were also investigated. In this akermanites crystal structures, the doping ions of Eu^{3+} will clearly substitute the alkaline earth metal (Ba^{2+}) ions. With an increase in the Eu^{3+} concentration, quenching of Eu^{3+} luminescence occurs. The critical quenching concentration of Eu^{3+} in $Ba_2MgSi_2O_7$: Eu^{3+} phosphor is determined as 0.05 mol. The mechanism of concentration quenching of $Ba_2MgSi_2O_7$: Eu^{3+} luminescence is energy transfer between Eu^{3+} ions casued by the dipole-dipole interaction. The CIE chromaticity coordinates of the optimized sample was calculated, (x, y) = (0.623, 0.376). The excitation spectrum couples well with the emission of UV-LED chips (380-410 nm). The results indicated that $Ba_2MgSi_2O_7$: Eu^{3+} is a potential red phosphor for phosphor-converted UV-LEDs.

Acknowledgement

This work was supported by the Natural Science Foundation of China (No.51002054), the Natural Science Foundation of Hubei Province of China (No.2008CB252), the Fundamental Research Funds for the Central Universities (C2009Q012) and by the Scientific Research Foundation for the Returned Overseas Chinese Scholar, State Education Ministry.

References

1. Schubert E.F., Kim J.K.: Science *308*, 1274 (2005).
2. Feldmann C., Jüstel T., Ronda C.R., Schmidt P.J.: Adv. Funct. Mater. *13*, 511 (2003).
3. Xie R.J., Hirosaki N.: Sci. Technol. Adv. Mater. *8*, 588 (2007).
4. Kim J.S., Jeon P.E., Park Y.H., Choi J.C., Park H.L., Kim G.C., Kim T.W.: Appl. Phys. Lett. *85*, 3696 (2004).
5. Nishida T., Ban T., Kobayashi N.: Appl. Phys. Lett. *82*, 3817 (2003).
6. Chou T.W., Mylswamy S., Liu R.S., Chuang S.Z.: Solid State Commun. *136*, 205 (2005).
7. Sivakuar V., Varadaraju U.V.: J. Electrochem. Soc. *152*, H168 (2005).
8. Yao S.S., Li Y.Y., Xue L.H., Yan Y.W.: Eur. Phys. J. Appl. Phys. *48* , 20602/1-4 (2009).
9. Yao S.S., Xue L.H., Yan Y.W., Li Y.Y., Yan M. F.: J. Ceram. Process. Res. *11*, 669 (2010).
10. Wan J.X., Wang Z.H., Chen X.Y., Mu L., Qian Y.T.: Eur. J. Inorg. Chem. *20*, 4031 (2005).
11. Wan J.X., Yao Y.W., Tang G.Y., Qian Y.T.: J. Nanosci Nanotechnol. *8*, 1449 (2008).
12. Yao S.S., Xue L.H., Yan Y.W., Yan M.F.: J. Am. Ceram. Soc. (2010). Doi: 10.1111/j.1551-2916.2010.04261.x
13. Yao S.S., Li Y.Y., Xue L.H., Yan Y.W.: Int. J. Appl. Ceram. Technol. (2009) Doi: 10.1111/j.1744-7402.2009.02447.x.
14. Satnta A.P.C., Teles S. F.: Spectra Lux Software v.2.0 Beta, Photo. Quânticao Nanodispositivos, Renami 2003.
15. Maia A.S., Stefani R., Kodaira C.A., Felinto M.F.C., Teotonio E.E. S., Felinto M.C.F.C.: Opt. Mater. *31*, 440 (2008).
16. Aitasalo T., Hölsä J., Laamanen T., Lastusaari M., Lehto L., Niittykoski J., Pellé F.: Z. Kristallogr. Suppl. *23*, 481 (2006).
17. Ekamabaram S., Maaza M.: J. Alloy. Compd. *395*, 132 (2005).
18. Kingsley J.J., Patil K.C.: Mater. Lett. *6*, 427 (1988).
19. Aitasalo T., Hölsä J., Laamanen T., Lastusaari M., Lehto L., Niittykoski J., Pellé F.: Ceramics-Silikáty *49*, 58 (2005).
20. Pires A.M., Davolos M.R.: Chem. Mater. *13*, 21 (2001).
21. Liebau F.: *Structural Chemistry of Silicates, Structure, Bonding and Classification,* Springer-Verlag, Berlin 1985.
22. Pei Z.W., Su Q., Zhang J.Y.: J. Alloys Compd. *198*, 51 (1998).
22. Van Uitert L.G.: J. Electrochem. Soc. *114*, 1048 (1967).
23. Ozawa L.J., Jaffe P.M.: J. Electrochem. Soc. *118*, 1678 (1971).
24. Kang Y.C., Chung Y.S., Park S. B.: J. Am. Ceram. Soc. *82*, 2056 (1999).
25. Carnall W.T., Fields P.R., Rajnak K.: J. Chem. Phys. *49*, 4450 (1968).
26. Judd B.R.: Phys. Rev.: Condens. Matter. *127*, 750 (1962).